International Journal of Innovation Engineering and Science Research
(ISSN: 2581-4591)
www.ijiesr.com

Extraction of Human Motion Parameters from Videos

[1]Daniela Hagiescu, [2]Felix Pirvan
[1,2]Advanced Slisys, Bucharest, Romania

[3]Lidia Dobrescu
[3]Faculty of Electronics, Telecommunication and Information Technology, University POLITEHNICA of Bucharest, Bucharest, Romania

ABSTRACT

Motion parameters of the human body can be powerful indicators for that person's activity, psychological or emotional state. As 3D coordinates of human body parts are often hard to collect, we propose a set of methods that take as input 2D video frames from an ordinary RGB camera. While this is obviously a limitation, we devised several ways to mitigate it and consequently extract useful information from the input video. We define 9 motion parameters that describe in various ways the person's motion: expansion, fluidity, characteristic energy, vivacity, symmetry, twist, dynamism, directness and periodicity. We believe this is a step into a better understanding of human motion, and can think of several direct applications.

Keywords—*motion parameter; movement parameter; human body; human motion; body part; body joint*

I. INTRODUCTION

Estimating human motion parameters has long been a subject of interest. Previous works have addressed the task from various directions, using various input data and trying to capture as much as possible the essence of the human motion.

One of the first attempts to analyze human motion [1] met the challenge of anatomical data gathering and obtained the weight and center of gravity position for various body parts using corpses. Voluntary motion of intermediate speed was found [2] to approach the smoothest trajectory, in terms of acceleration's rate of change (jerk), being motivated by neuro-muscular considerations. The study of the voluntary arm motion coordination [3] showed that the trajectory yielding the best performance can be determined by the dynamic optimization theory and minimizes the square magnitude of the jerk. The role of gestures in the non-verbal communication process [4] is explored in relation with dance and music as ideal conveyors of expressive and emotional content. The influence of basic emotions, happiness and sadness, on a person's dance [5] revealed differences in the body motion which were captured through motion parameters. 3D motion data captured with a RGB-D sensor was used to extract motion features and parameters [6], serving for human emotion recognition.

Our contributions are the following:

- New method of 2D trajectory smoothing, aimed at reducing the square of the jerks, without using predefined intermediary points and keeping the overall trajectory shape (no curve flattening)
- Definition of 9 motion parameters, extractable from 2D coordinates: expansion, fluidity, characteristic energy, vivacity, symmetry, twist, dynamism, directness and periodicity; although a few of them have been defined before in the 3D case, we adapted those definitions to the 2D case, which is more common

II. PRELIMINARIES

We use a Web camera to capture 17 video sequences. In each video, the same person is performing a dance in a particular dance style (Ballet, Freestyler, Macarena, Lambada and others). We used a wide variety of dance styles to be able to compare the motion parameters between them and draw conclusions about the particular features of each dance style. All videos are recorded at 30 frames per second and have 2000 frames, or roughly 66 seconds in length. To obtain the positions of the body joints, we use Open Pose [7], which is a method based on a deep neural network and has shown some of the best results for this task. It predicts 14 joints: head top, neck, shoulders, elbows, wrists, hips, knees and ankles. In fig. 1, we marked the predicted joints and the limbs obtained by connecting them.

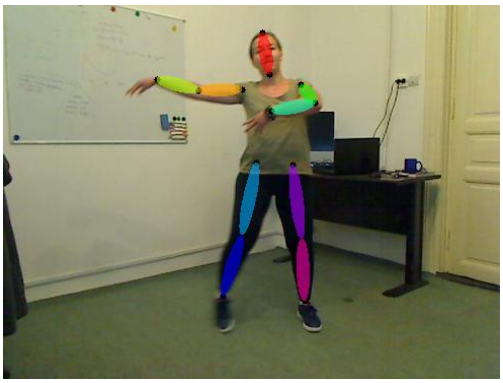

Fig. 1 Joints detected by OpenPose and limbs between them

For some images, skeleton detection can produce more than one skeleton. We are only interested in a single skeleton, so the first step is to filter out the unwanted skeletons. We first ensure that we have only one skeleton in the first frame of every video. Then for each frame with multiple skeletons, we compute the sum of distances from each joint to the corresponding joint of the skeleton in the previous frame and we keep the skeleton with the smallest sum. In other words, we keep the skeleton spatially closest to the unique skeleton in the previous frame.

III. TRAJECTORY SMOOTHING

The detection of joints faces a large array of difficult cases. Body part similarity can lead to confusion between left and right limbs. The fast motion of the person can blur the joints and therefore make the joint position unclear. Hidden joints are harder to estimate. All these cases yield perturbations in the series of joint positions.

The simplest method to smooth a data series is the moving average. This method replaces each value in the series with the average over an interval around that value. The filter Savitzky-Golay [8] is a generalization of the moving average that obtains the filter coefficients using a polynomial for a linear least squares fit of the data. Local Regresion Smoothing [9] uses locally weighted scatter plots with polynomial of first or second degree.

We smooth the joint trajectories by reducing the instantaneous acceleration. Our method is based on the actual meaning of the data. Body joints that describe the trajectories are physically constrained by the body muscles which cannot make too sharp changes in speed, so when smoothing we aim at minimizing the joint accelerations. In fig. 2, we represent a fragment from a joint trajectory. Let A, B, C, D, E be the joint positions in succesive frames. Let C', D', E' be the reflections of A with respect to B, of B with respect to C, and of C with respect to D, respectively. C', D', E' are the expected positions for C, D, E under uniform motion. In the physical interpretation, AB, BC, CD and DE are the velocities of the joint between two consecutive frames, while C'C, D'D and E'E are the accelerations of the joint in the points C, D and E respectively. In order to smooth the trajectory in the current point C, we move this point towards C', thus reducing the acceleration. This move also has the desired effects of a change in the position of D' twice as big towards D, and a change in the position of E' towards E. We continue to move C towards C', as long as the sum of squares of the accelerations decreases. If C reaches C', we

stop and continue the same procedure for the next point D, taking into account the accelerations D'D, E'E and F'F.

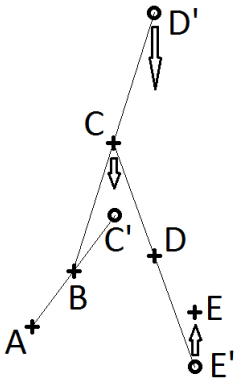

Fig. 2 Trajectory smoothing. Crosses represent joint positions, circles represent positions that would cancel the acceleration for each 3-point segment. Moving point C would change the positions of D' and E' in the desired directions, thus reducing the sum of squares of the accelerations

In fig. 3, we represented a practical example of trajectory smoothing. The series of accelerations is represented on the first row, and values obtained after smoothing, under the bars. The method gradually updates the values, in groups of 3.

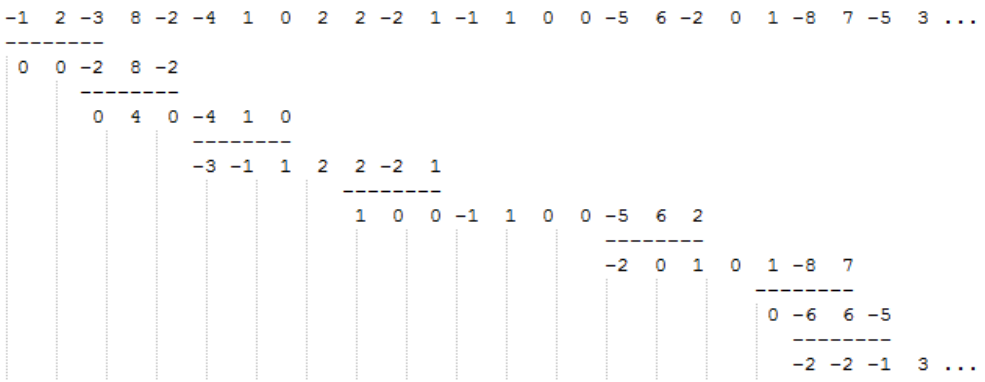

Fig. 3 Trajectory smoothing. The first row represents the successive accelerations of a joint. Below the bars, there are the smoothed accelerations. The sum of squares of all the accelerations goes down from 327 to 57, while the sum of their absolute values decreases from 67 to 25.

In fig. 4, we present a real case scenario, where the trajectory of the right wrist was smoothed. It can be seen that motion blur affects the detection, but trajectory smoothing follows more naturally the motion of the wrist.

Fig. 4 Trajectory smoothing. The detected right wrist (left side of the image) is represented by a black dot, while the smoothed trajectory positions are represented by a red dot. The dots are overlapping in the initial and final positions, while there is significant distance between them in the frames in-between.

IV. The Motion Parameters

Expansion, a parameter describing the quality of the motion, was previously defined [5] between wrists and elbows, on one hand, and the body center, on the other hand. We adapted this definition to our 2D data, also taking into account the variation of the distance between person and camera. We normalized the values obtained for the expansion and integrated them over an interval of several seconds, to cancel out the momentary variations. Let A be the wrist, B – the elbow, C – the shoulder, and D – the hip on the same side of the body. We compute the expansion as:

$$E = \frac{AD}{AB + BC + CD} \quad (1)$$

As can be deduced from the formula, the expansion takes values in [0, 1]. When the wrist touches the hip, the expansion is 0. When the arm is extended upwards and all four joints (hip, shoulder, elbow and wrist) are collinear, the expansion is 1. In order to reduce the errors due to foreshortening of limbs in the projection plane, we compute this parameter for the left side of the body, as well as for the right side, and take the expansion of the body to be the maximum of the two. In fig. 5, we represented the expansion extracted from three different dances: Ballet, Freestyler and Macarena. The graph shows that, although there is variation within each dance, the Ballet expansion is generally the highest, while the Freestyler expansion is the lowest and has the smallest variance. Also, within one dance style, there are periods of relatively constant expansion, reflecting specific dance routines. This can best be observed in the Ballet graph, which has roughly 3 such periods, the first with a high expansion, the second with lower expansion, and the third with very high expansion.

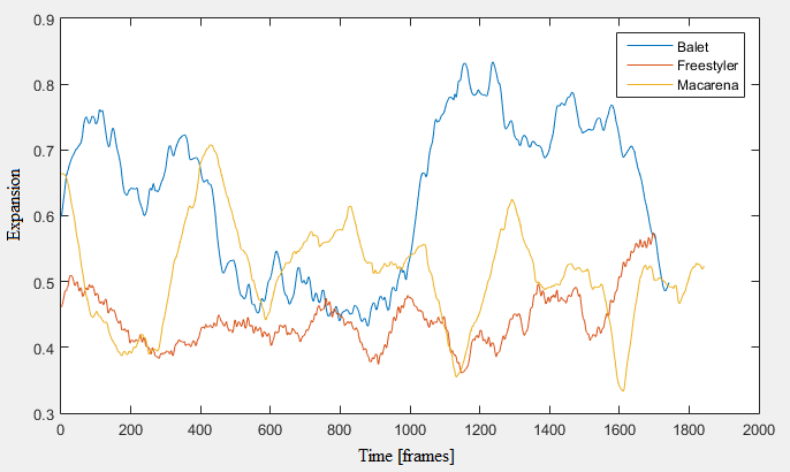

Fig. 5 The expansion of the body during three different dance styles, as a function of time. Each moment of time is a video frame.

Some motion parameters describe well a certain part of the motion. When we talk about wide gestures or a fluid motion, we mean not just spatial extent, but also temporal, i.e. the time interval (number of frames) during which that gesture (motion segment) takes place. We define the **anchors** of a motion as the points where the trajectory of a joint either stop, or perform a sudden direction change, of at least 90^0 . The motion anchors split the joint trajectory in **motion segments**, characterized by a certain motion continuity. During a motion segment, the direction can change by any amount, but not suddenly. A motion segment can have any length, defined as the number of frames between the final anchor and the initial anchor. Fig. 6 shows a joint trajectory during 16 frames and has the motion anchors painted red.

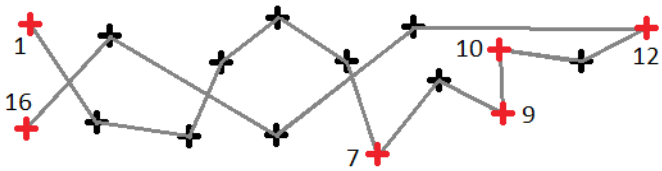

Fig. 6 The trajectory of a joint during 16 frames. The motion anchors are represented in red, defining 5 motion segments, between the frames 1-7, 7-9, 9-10, 10-12 and 12-16. Each motion anchor marks a change in direction of more than 90^0 .

A motion is fluid if it has only small instantaneous changes in acceleration, called jerks. Because the motion as a whole has inherent jerks at the anchors, we analyze the fluidity during the motion segments, as a property of each segment. For a rectilinear motion between two points, the position of intermediary points that minimize the jerk can be computed, given the initial and final velocities and accelerations are zero. [2] But for a multidimensional motion, the formula can be applied only with the additional condition that the trajectory passes through a certain point at a certain moment [3], which makes it lose its generality. In our situation, we don't have mandatory intermediary points, and without them, the trajectory that minimizes the jerk between any two points would be the straight line between them. So we cannot minimize the jerk without reducing the trajectory to a straight line.

The fluidity index was defined in [6] as the inverse of the jerk, integrated over the length of the motion segment. For the discrete case of the pixel-level trajectory, this formula yields too small values, because the smallest non-zero jerk is 1, for which it would result a fluidity index of 0.5, too small for a small jerk. Thus, we define the **fluidity** as the square root of the inverse of the average jerk of a motion segment, scaled to take values in [0, 1].

$$F = \frac{1}{\sqrt{j+1}} \tag{2}$$

It approaches zero when the jerk is very high. It is equal to 1 when the jerk is equal to 0. As the jerk depends on the joint position in 4 consecutive frames, the fluidity can only describe motion segments of length at least 3. Fig. 7 shows the average lengths of the motion segments of each joint, for three selected dance videos. The head and arm joints in the ballet video have much longer motion segments, reflecting the wider and slower gestures, especially of the upper body parts.

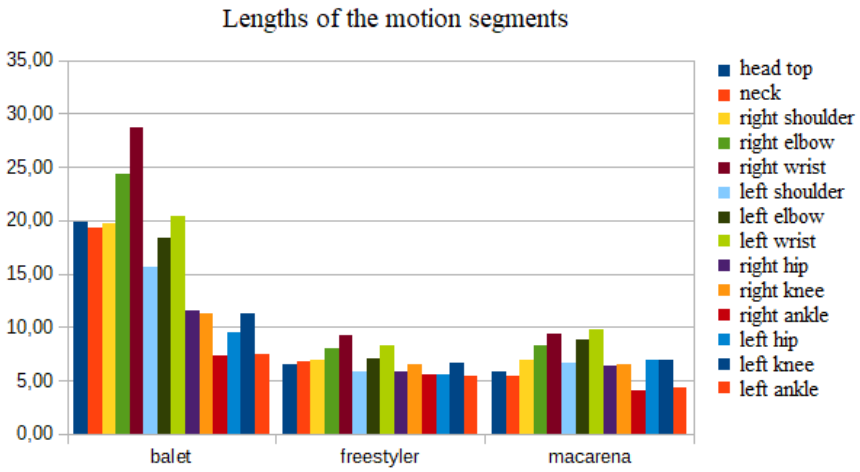

Fig. 7 Average lengths of the motion segments for three dance videos, expressed in number of frames

Fig. 8 shows the average fluidity of three dance videos. It can be seen that Ballet is the most fluid dance, while Freestyler is the least fluid. The graph also shows a relative pattern in the fluidity of the joints. The wrists are the least fluid of all joints, because they can move more freely and thus more

sudden than the other body joints, which are stronger connected and thus have more motion constraints and fewer degrees of freedom. In fact, there is a decrease in fluidity from shoulder to elbow to wrist. Also, the head top is slightly less fluid than the neck, while the lower body joints have similar fluidity during the same dance style.

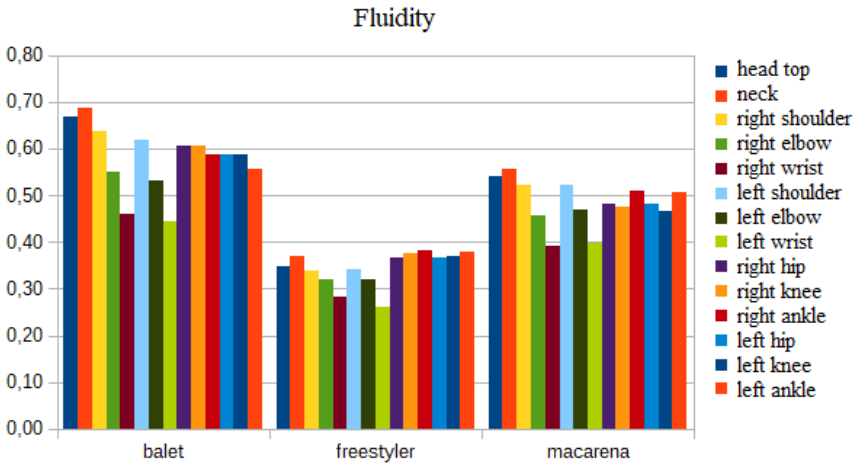

Fig. 8 Fluidity of the motion segments for three dance videos

Fig. 9 shows the fluidity as a function of the motion segment length. The analyzed joint is the right hip from the Ballet video, which has an average fluidity of about 0.6, as it can be seen in fig. 8. Each blue circle represents a motion segment. While the motion segments can vary in length from 3 to 48, shorter lengths, in the range [3, 7], are better represented than longer ones, which was expected. Also, the shorter motion segments have more fluidity variance. The red asterisks mark the average fluidity for each motion segment length. These highlight the fact that the fluidity of a certain joint in a certain dance style does not depend on the motion segment length: in this case, they are all close to 0.6, the global average.

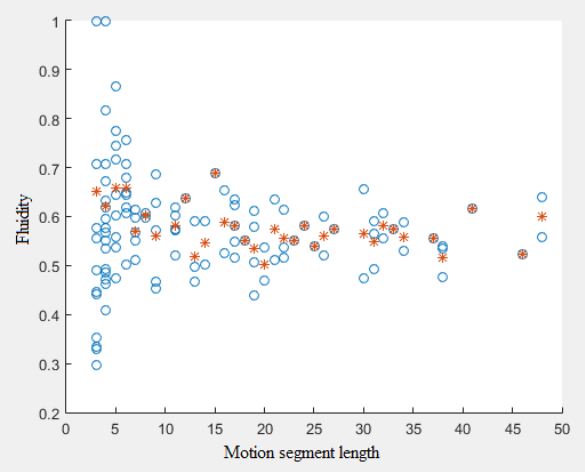

Fig. 9 Fluidity as a function of motion segment length. Each segment is represented by a blue circle, while each red asterisk represents the average fluidity of segments of the same length.

The joints define the body parts that connect them: trunk (quadrilateral defined by shoulders and hips), head, upper arms, forearms, thighs, calves. The kinetic energy of a body articulated from rigid parts is the sum of the kinetic energies of its parts. We don't know the mass of the person in question, but we can compute its **characteristic energy** (energy per mass unit). We need to know the fraction of each body part of the total body mass, as well as the position of the center of gravity of each body part relative to one of its extremities. We used the average values computed from a sample of 135 corpses

(35 males and 100 females). [1] Since we only have 2D coordinates, we are only computing the projection of the total characteristic energy on the projection plane. We use this formula for the characteristic energy:

$$\varepsilon = \frac{E}{m} = \sum_p \left(\frac{\frac{m_p}{m} * v_p^2}{2}\right) \quad (3)$$

where E – translational kinetic energy, m – body mass, p – body part, m_p – mass of the body part, v_p – velocity of the body part.

The velocity of a body part acts in its center of gravity and can be computed from the velocities of the joints at the extremities of the body part. For the trunk, we take the extreme points as the middle of the shoulder line and the middle of the hip line.

$$\vec{v}_p = \vec{v}_{p_1} + (\vec{v}_{p_2} - \vec{v}_{p_1}) * \left(\frac{G - P_1}{P_2 - P_1}\right) \quad (4)$$

where v_{p1}, v_{p2} – velocities of the body part extremities, G – position of the center of gravity of the body part, P_1, P_2 – positions of the extremities of the body part.

Similar to the characteristic energy, we compute the **vivacity** or characteristic moment (moment per mass unit). The moment of the whole body is the sum of the moments of all the component parts. Since we only have 2D coordinates, we are only computing the projection of the total vivacity on the projection plane. We use this formula for the vivacity:

$$\pi = \frac{p}{m} = \sum_i \left(\frac{m_i}{m} * v_i\right) \quad (5)$$

where p – moment, m – body mass, i – body part, m_i – mass of the body part, v_i – velocity of the body part.

The **symmetry** of the motion can be approached in several ways. To compute it relative to the section planes of the human body (frontal, sagittal and transversal), as in [6], we need the 3D joint coordinates. Of the 2D coordinates we have, the vertical coordinate is invariant to the predominant rotation of a person relative to the camera (in the horizontal plane), while the horizontal coordinate is heavily affected by this rotation. Therefore, we only take into account the vertical coordinate to compute the symmetry. A symmetric motion can be simultaneous, but it can also be alternating. For example, for an alternating raise of the hands, most of the frames contain asymmetric positions, although the motion as a whole can be considered symmetric. We define the relative height of the wrist with respect to the shoulder on the same side, as:

$$h_{rel} = \frac{\frac{y_A - y_C}{AB + BC} + 1}{2} \quad (6)$$

where A, B, C – positions of the shoulder, elbow and wrist, respectively, y_A, y_C – vertical coordinates of the shoulder and wrist (measured from the upper side of the image).

The relative height takes values in [0, 1]. When the arm hangs perfectly downwards, AB + BC = y_C - y_A, therefore h_{rel} = 0. When the arm is stretched perfectly upwards, AB + BC = y_A - y_C, therefore h_{rel} = 1. And when the whole arm is on the same horizontal with the shoulder, either stretched or flexed, y_A = y_C, therefore h_{rel} = 0.5. Integrating the left and right relative heights over several frames, to take into account the alternating motions, we obtain $H_{rel}(L)$ and $H_{rel}(R)$. The closest the integrated relative heights are, the more symmetric the motion. So we use this formula for the symmetry:

$$S = 1 - |H_{rel}(L) - H_{rel}(R)| \quad (7)$$

We compute the symmetries of the ankles in the same manner, using hips and knees instead of shoulders and elbows. Fig. 10 represents the symmetries computed for two dance styles, Ballet and Freestyler. Relative heights were integrated over 150 frames (5 seconds). The graphs show that wrist symmetry is greater for the Freestyler dance (over 92%), while the ankle symmetry is comparable for the two dance styles (over 96% in both cases). In general, ankle symmetry will always be close to 1 if both ankles stay mostly close to the ground.

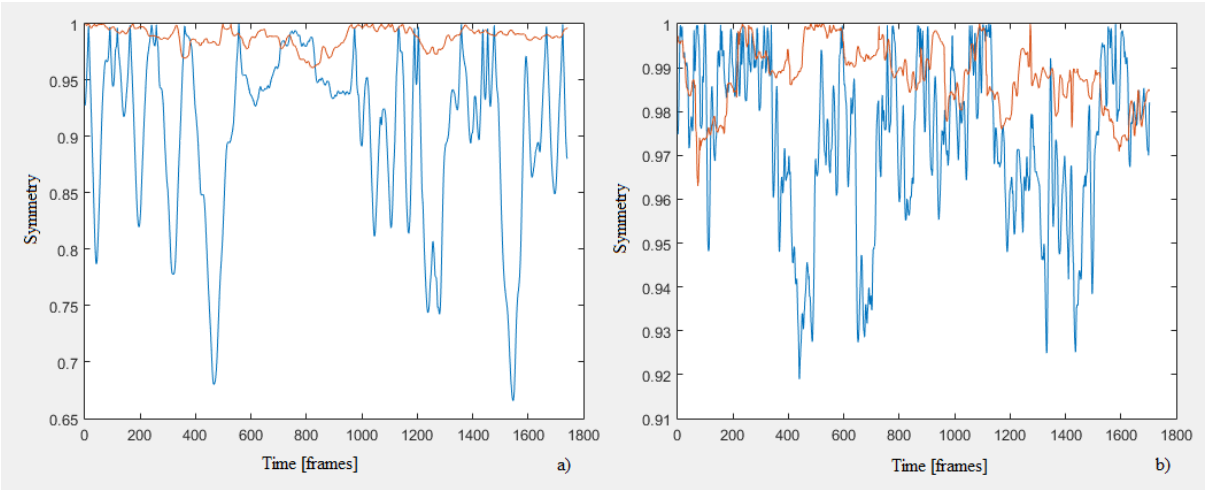

Fig. 10 Symmetries of wrists (blue) and ankles (red) computed from two dance videos, Ballet (a) and Freestyler (b). Note the different vertical scales

We define three types of tilts: head tilt relative to the trunk (in the range [0, 90] degrees), trunk tilt relative to the vertical (in the range [0, 180] degrees) and hips tilt relative to horizontal (in the range [0, 90] degrees). These parameters combined can offer hints about the overall body **twist**. The head direction is the line between the head top and the neck. The trunk is the quadrilateral defined by the shoulders and hips and its direction runs from the middle of the shoulder line to the middle of the hip line. Due to limits imposed by the 2D projection, we can only compute these values in the projection plane. Foreshortenings of the limbs on the axis person-camera can affect the tilts, the hip line being especially susceptible of abnormal high tilts when the person is viewed from the side and the horizontal hip coordinates almost coincide. Therefore, when computing the overall body twist, we weight the hips tilt by the ratio of the hip line length to the maximum hip line length over the last few seconds. With this precaution, the formula for the twist is:

$$T = (t_1 / 90 + t_2 / 180 + t_3 * d_h / D_h / 90) / 3 \quad (8)$$

where t_1, t_2, t_3 – head tilt, trunk tilt, hips tilt, respectively, d_h – distance between the hips, D_h – maximal distance between the hips over the last few seconds.

All tilts are scaled to their respective range, to bring the overall body twist in [0, 1]. A person in a upward vertical position has all the tilts equal to 0, so the twist is also 0. A person performing a complicated break dance move, with the trunk upside-down, and with the head and hips tilted at 90 degrees relative to the trunk would have all tilts equal to their respective maximal angles, and the twist equal to 1.

Often a person, during an activity (dance or other), changes her/his support leg and moves her/his center of gravity from one leg to another, passing through poses where the equilibrium is dynamic. We define the **dynamism** as the degree of instability of a certain pose. It depends on the horizontal distance between the center of gravity and the edge of the support base, as well as on distance that the free leg has to cover in order to recover the stable equilibrium. In the context of our data (2D coordinates of the body joints), we consider the ankles as the points of support. Also, the ankles will rarely have the same vertical coordinate, so almost always it will appear to be a single point of support, the lowest ankle. When, in reality, the person has both legs on the ground and the center of gravity falls

between them, the highest ankle will appear close to the height of the support ankle and therefore will have to cover only a small distance to recover the apparent stable equilibrium.

Fig. 11 shows the three possible situations that can arise with respect to the relative positions of the center of gravity (G) and the two ankles, inferior (J) and superior (S): G falls on the side of the J, G falls between J and S, G falls on the side of S. Let G' and S' be the projections of G and S on the horizontal line that passes through J.

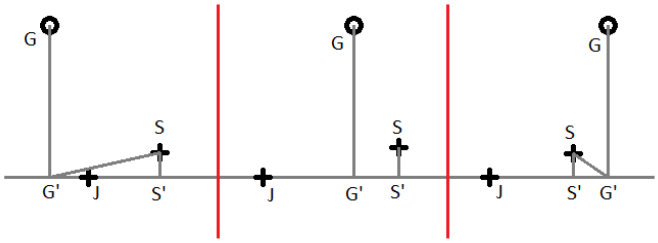

Fig. 11 The three cases that can occur with respect to the horizontal position of the center of gravity (G) relative to the inferior (J) and superior (S) ankles. G' and S' are the projections of G and S on the horizontal of J

We define the dynamism as:

$$D = \begin{cases} JG' * SS' & if\ G'\ between\ J\ and\ S' \\ JG' * SG' & otherwise \end{cases} \quad (9)$$

The case when G falls between J and S (G' is between J and S') is represented in the central panel of fig. 11 and S needs only to move to S' to reach the stable equilibrium. Otherwise, G falls outside of the segment JS' and S needs to move to G' to reestablish the stable equilibrium, as the lateral panels of fig. 11 show. If G' = S', the two branches of the formula become identical. If G' = J, then D = 0, because the center of gravity is right above the support ankle and the equilibrium is stable. If S = S' and G' between S and J, then D = 0, because the two ankles are on the same horizontal line and the center of gravity falls inside the support base.

We estimated the center of gravity based on average human data [1] for the mass of each limb relative to the total body mass and on the position of the center of gravity of each limb relative to its proximal extremity. We computed the dynamism for the dance videos Ballet, Freestyler and Macarena. Because dynamism can have very big values in case of bad joint detection, a video sequence is better described by the median of dynamism than by its mean. The results are in presented in Table I and match the intuitive observations: Macarena style is mostly static, with both feet almost always on the ground, Ballet style include legs in the air or jumps from time to time, while Freestyler dance is very dynamic, with lots of jumps from one leg to another.

TABLE I. DYNAMISM

Dance	Median Dynamism
Ballet	154
Freestyler	320
Macarena	84

For each motion segment, **directness** is the ratio between the length of the total displacement and the distance covered by the joint during that segment. [4] The formula for directness is:

$$d = sum(P_iP_{i+1}) / P_0P_n \quad (10)$$

where i – index of frame in the segment, in [0, n-1], P_i – position of joint at frame i.

Directness belongs to [0, 1]. It is equal to 0 when the segment starts and finishes in the same point and it is equal to 1 when the segment is a straight line. For example, in fig. 6, directness of the last motion segment is $(P_{12}P_{13} + P_{13}P_{14} + P_{14}P_{15} + P_{15}P_{16}) / P_{12}P_{16}$.

Periodicity was analyzed with respect to the frontal, sagittal and transversal planes, given the 3D coordinates of the joints. [6] As we only have 2D coordinates, we only take into account the vertical motion, which is invariant to the predominant rotation of a person, in the horizontal plane. In fact, almost any horizontal motion of a person implies an associated vertical motion, due to the need for a support base and to the way the body is articulated.

We compute the periodicity using the Fourier transform, whose power spectrum highlights the main frequencies of a signal. The periods can then be obtained from those main frequencies. To apply the Fourier transform on the time-series of the joint coordinates, these need to be normalized first, otherwise the maximal value of the power spectrum will correspond to the frequency zero, representing the mean of the signal values. In addition, the joint positions are harder to interpret, as they do not have a well defined range. Although constrained within the image size, the actual trajectory of a joint is hard to predict or evaluate. Instead, we use the instantaneous velocities, equivalent to the differences in position from one frame to the next. These have a natural near-zero mean, because the probability that the velocity takes positive or negative values is the same, and have a predictable distribution, as the small values are dominant and the very big outlier values can be considered detection errors. We compute periodicity for each joint, over a certain time window. The window size does not affect the outcome, as long as it is not too short to catch the short periods. However, a window too long introduces a lag in the reaction time in case of a change in periodicity over time. We found that a 5 seconds (150 frames at 30 fps) window is appropriate for most purposes. We also perform the necessary scaling to express the periodicity in beats per minute, so its formula is:

$$P = [\frac{60\,n\,i}{N}] \tag{11}$$

where n – number of frames per second, i – index of the maximal spectral density, N – number of frames of the window.

V. Conclusions adn Further Work

We computed 9 human motion parameters: expansion, fluidity, characteristic energy, vivacity, symmetry, twist, dynamism, directness and periodicity. Some of them (expansion, dynamism) are computed for each individual image, others (fluidity, directness) are computed for each motion segment, while the rest need a sequence of two or more video frames.

As different human activities are likely to be reflected in different overall motion parameters, one could discriminate between human activities based on these parameters. As we saw in our analysis, even different styles of dance can have very different motion parameters.

Motion parameters can be a good indicator of a person's psychological or emotional state. For example, big values of energy, vivacity or dynamism can suggest a good state of mind, while small values can hint to apathy or bad mood. More research is needed in this area.

By capturing the motion parameters from a dancing person, one could generate music in real-time that is more appropriate to that person's dance style. For example, the person dances slower than the music rhythm, so the music can adapt to that person rhythm. The music can also take into account the estimated emotional state of the dancing person, to match it more closely. For example, the music can become more energetic or more dynamic or more fluid, depending on those specific parameters.

Acknowledgment

The results presented in this work concerns the research carried out for the "SENTIR" research project, co-financed through the European Regional Development Fund, POC–A.1–A1.2.1–D–2015 grant,

research, development and innovation supporting economic competitiveness and the development of businesses.

REFERENCES

[1] Z. Cao, T. Simon, S.-E. Wei, Y. Sheikh, "Realtime Multi-Person 2D Pose Estimation using Part Affinity Fields", Conference on Computer Vision and Pattern Recognition (CVPR), arXiv:1611.08050, 2017

[2] A. Savitzky, M. J. E. Golay, "Smoothing and Differentiation of Data by Simplified Least Squares Procedures", in Analytical Chemistry, 36 (8), pp. 1627-1639, 1964

[3] J. Fox, S. Weisberg, "An R Companion to Applied Regression", SAGE Publications, 2018

[4] E. Van Dyck, P. J. Maes, J. Hargreaves, M. Lesaffre, M. Leman, "Expressing Induced Emotions Through Free Dance Movement", Nonverbal Behav 37, pp. 175-190, 2013

[5] N. Hogan, "An Organizing Principle for a Class of Voluntary Movements", The Journal of Neuroscience, vol. 4, no. 11, November 1984

[6] T. Flash, N. Hogan, "The Coordination of Arm Movements. An Experimentally Confirmed Mathematical Model", The Journal of Neuroscience, vol. 5, no. 7, July 1985

[7] S. Piana, A. Staglianò, F. Odone, A. Camurri, "Adaptive Body Gesture Representation for Automatic Emotion Recognition", ACM Transactions on Interactive Intelligent Systems, vol. 6, issue 1, pp. 1-31, May 2016

[8] S. Plagenhoef, F. Gaynor Evans, T. Abdelnour, "Anatomical Data for Analyzing Human Motion", Research Quarterly for Exercise and Sport, vol. 54, no. 2, 1983

[9] A. Camurri, B. Mazzarino, M. Ricchetti, R. Timmers, G. Volpe, "Multimodal Analysis fo Expressive Gesture in Music and Dance Performances", Gesture-Based Communication in Human-Computer Interaction Conference, 5th International Gesture Workshop, Genova, April 2003